

Date of publication xxxx 00, 0000, date of current version xxxx 00, 0000.

Digital Object Identifier 10.1109/ACCESS.2017.Doi Number

# Design of a $PI^\alpha$ fractional controller for the robust control of the steam pressure in the steam drum of a bagasse-fired boiler

Vicente Feliu-Batlle<sup>1</sup>, (Senior Member, IEEE), Raul Rivas-Perez<sup>2</sup>, and Fernando Castillo-García<sup>3</sup>

<sup>1</sup>Escuela Técnica Superior de Ingenieros Industriales, and Instituto de Investigaciones Energéticas y Aplicaciones Industriales Universidad de Castilla-La Mancha (UCLM), Edificio Politécnico, Ave. José Cela, 3, C.P. 13071, Ciudad Real, España

<sup>2</sup> Universidad Tecnológica de la Habana José Antonio Echeverría (CUJAE), Calle 114 No 11901, Marianao, La Habana, C.P. 19390, Cuba

<sup>3</sup> School of Industrial and Aerospace Engineering, University of Castilla-La Mancha, C.P. 45071 Toledo, Spain

Corresponding authors: Vicente Feliu-Batlle and Raul Rivas-Perez (e-mail: vicente.feliu@uclm.es; raul\_rivas\_perez@yahoo.es).

This work was supported in part by the University of Castilla-La Mancha under Project 2020-GRIN-29090, and in part by the European Social Fund (FEDER, EU).

**ABSTRACT** This paper proposes the design of a  $PI^\alpha$  fractional robust controller with which to regulate the steam pressure in the steam drum of a bagasse-fired boiler. The dynamic behavior of this process was identified by means of experimentation. This identification procedure yielded an equivalent third order plus time delay model, and showed wide process static gain variations. We, therefore, propose a new method with which to design fractional-order robust controllers for this kind of processes. This method is based on the exact attainment of certain nominal time specifications while using one of the parameters of the controller to maximize the gain margin. The controller attained was shown to significantly outperform the robustness achieved by using  $PI$  or  $PID$  controllers, in the sense of reducing the Integral Absolute Error ( $IAE$ ) and improving the steam pressure uniformity.

**INDEX TERMS** Steam pressure control, robust fractional-order controller, bagasse-fired boiler, system identification

## I. INTRODUCTION

The sugarcane industry is regarded as one of the world's oldest industries, in which sugarcane bagasse is largely used as a combustible fuel to generate electrical and thermal energy for this industrial process [1], [2]. This industry involves three basic processes: the cultivation of cane, the milling of the sugarcane to extract the juice, and the industrial conversion of this juice into raw sugar [3]. Bagasse is a by-product of the grinding operation [4]. Traditional sugarcane factories are characterized by their high energy consumption and pollution of the environment, largely owing to their low-efficiency technology [5]. The increase in the energy crisis, high competitiveness in energy markets and strong environmental demands have, therefore, led the research aimed at increasing energy efficiency and reducing the impact that the industrial activity associated with sugarcane has on the environment to acquire great relevance and scientific-technical importance [6], [7].

The bagasse-fired boiler is an essential component of this

industry since bagasse, which is a waste product of the industry itself, is used as fuel, thus guaranteeing relatively economic energy production [8]. The conditions of high pressure and temperature under which this boiler is operated also make it one of the most potentially dangerous pieces of equipment in this industry [9], and one of the most energy wasting units. Studies related to the design of effective controllers for bagasse fired boilers are, therefore, imperative [9], [10].

Bagasse-fired boilers are characterized by their complex dynamic behavior: time-varying parameters and various interacting processes that are usually controlled independently by conventional  $PID$  controllers [10]. If these boilers are to operate in a highly efficient manner, it is necessary to [11]–[13]: 1) guarantee that the amount of bagasse necessary to keep the steam pressure within the required limits is burned, independently of the load variations; and 2) maintain a correct air/bagasse ratio, which will enable a complete combustion within the design

limits of the boiler. These requirements cannot be guaranteed if there is no effective steam pressure control in the steam drum of the boiler [14].

The bagasse-fired boilers in the sugarcane industry are required to operate at constant pressure [3], and several strategies for steam pressure control in the steam drum of these boilers have, therefore, been proposed for this purpose [15]–[23]. The most popular and widespread strategy is based on conventional  $PID$  controllers (analog or discrete) owing to their simple structure, flexibility, easy tuning and general robustness properties [5], [21]. However, some studies have shown that simple  $PID$  controllers do not perform well when the dynamic behavior of this kind of processes is characterized by time delay, time-varying parameters and unmeasured disturbances [15], [24]–[26]. These result in a large steam pressure settling time in the steam drum, which leads to excessive bagasse consumption and, therefore, inadequate combustion and great environmental pollution. Any controller designed for this purpose should consequently have an adequate robustness with which to deal with the steam drum dynamics.

During the past three decades, the subject of fractional calculus, i.e., the calculation of integrals and derivatives of any arbitrary real or complex order, has gained considerable popularity and importance, principally owing to its demonstrated applications in diverse and widespread fields of science and engineering [27], [28]. Fractional order operators have, therefore, also been applied with satisfactory results to model and control processes with complex dynamic behaviors [29]–[33].

The concept of extending classical integer order operators to non-integer order ones is by no means new. For example, [27] mentions that the earliest systematic studies, which were carried out by Liouville, Riemann, and Holmgren, date from the beginning and middle of the 19th century. The significance of the application of fractional order operators to the design of control systems is based on a generalization of the classical integer order control theory, which yields more adequate models of the processes and control systems that have a better performance.

The fractional order basic operator is represented as  ${}_a D_t^\alpha$ , where  $a$  and  $t$  are the limits and  $\alpha$  ( $\alpha \in \mathbb{R}$ ) is the order of the operator [28]. In this operator,  $\alpha > 0$  represents a fractional derivative, and  $\alpha < 0$  a fractional integral. In the Laplace domain, this operator corresponds to a fractional-order differentiator or integrator  $s^\alpha$  (provided that initial conditions are zero). The frequency characteristics of this operator is, therefore,  $(j\omega)^\alpha$  [27].

The robustness of  $PID$  controllers can be enhanced by means of their generalization to  $PI^\alpha D^\lambda$  fractional-order controllers by involving an integrator of order  $\alpha$  and a differentiator of order  $\lambda$  [28]. Fractional order controllers ( $PI^\alpha D^\lambda$ ) have received a considerable amount of attention, e.g. [34]–[43].

The qualitative behavior and the robustness of industrial

$PID$  controllers when applied to the steam pressure control of the steam drums of bagasse-fired boilers can consequently be improved through the design of  $PI^\alpha D^\lambda$  controllers. This paper concentrates on the design of a reduced version of a  $PI^\alpha D^\lambda$  controller: the fractional-order  $PI^\alpha$  controller.

The objectives of this paper are: 1) to propose a systematic and analytic method with which to design a robust  $PI^\alpha$  controller that will guarantee a minimum performance when the steam pressure dynamics changes as a result of variations in bagasse calorific values, 2) to make a comparison among the robustness of this  $PI^\alpha$  controller and that of another equivalent conventional controllers ( $PI$  and  $PID$ ) by means of computer simulations.

The main contribution of this paper is the proposal of a robust  $PI^\alpha$  controller with which to control the steam pressure in the steam drum of a bagasse-fired boiler, for which very satisfactory results have been obtained. A practical solution to the complex problem of designing effective controllers for bagasse-fired boilers that have some dynamics uncertainties and which outperform conventional  $PI$  and  $PID$  controllers is, therefore, provided. All the modeling and control methodologies shown in this paper have been carried out for a real industrial bagasse-fired boiler, whose nominal dynamics and ranges of parameter variations have been determined experimentally.

This paper is organized as follows. A linear dynamic model of the steam pressure in the steam drum of this boiler is obtained in Section 2. A method with which to design  $PI^\alpha$  controllers for this process is proposed in Section 3. Simulations of this controller when regulating the steam pressure of the process in the case of there being uncertainties in some parameters are carried out in Section 4. Moreover, this section discusses the results obtained by this controller when compared to other standard controllers. Finally, some conclusions are drawn in Section 5.

## II. SYSTEM IDENTIFICATION OF STEAM PRESSURE IN THE DRUM OF A BAGASSE-FIRED BOILER

### A. DESCRIPTION OF BAGASSE-FIRED BOILER

The study presented in this paper is based on the bagasse-fired boiler of the ‘30 de Noviembre’ sugarcane industry in the province of Artemisa, Cuba. This industry operates as a cogeneration facility, providing steam to the sugar mill while simultaneously providing electric power to the grid. The boiler comprises water tubes and can generate up to 80 T/h of steam with a maximum pressure of 30 kg/cm<sup>2</sup>.

The main purpose of the bagasse-fired boiler is to convert the energy contained in the bagasse into heat energy, which is then transferred to water for its conversion into steam at a desired temperature and pressure [3], [8]. This steam is subsequently used to generate mechanical and electrical energy, or to feed other equipment and processes

of the industry itself. Fig. 1 shows a view of this kind of boilers.



**FIGURE 1.** View of a bagasse-fired boiler.

Bagasse is a fuel of varying composition, consistency, and calorific value [12], [39]. These characteristics depend on the climate, type of soil upon which the sugarcane is grown, variety of sugar cane, harvesting method, amount of sugar cane washing, and the efficiency of the milling plant.

After being dried and crushed, the bagasse is carried on a conveyor mat to the rotary feeders (known as bagasse feeders) which are those that introduce the necessary bagasse into the furnace for its combustion [3]. These feeders have motors that turn two rollers whose rotation speed is proportional to the mass flow of the bagasse entering the furnace.

The steam pressure required in the steam drum of the boiler determines the mass flow of the bagasse entering the furnace and, consequently, the speed of the motors of the rotary feeders. The steam drum is the upper drum of the boiler in which the separation of water and steam occurs.

The speed of the motors in these devices is regulated through the use of Variable Frequency Drives (VFD) and can reach between 7 rpm at 25 Hz and 17 rpm at 60 Hz. The nominal operation steam pressure in the steam drum of the boiler is 23 kgf/cm<sup>2</sup>, which is attained with the combustion of a nominal bagasse flow of 8000 kg/h.

### B. DYNAMIC MATHEMATICAL MODEL

One of the main variables that must be controlled in this type of plants is the steam pressure in the steam drum of the bagasse-fired boiler, because it is an indicator of the energy balance between the steam that is generated and that which is demanded [44]–[46]. This pressure is proportional to the amount of steam generated and indicates the output energy [47], while the bagasse flow represents the input energy [8]. The mathematical model will, therefore, have the steam pressure variation in the steam drum of the boiler ( $\Delta y(t)$ ) as the output variable and the % of the speed variation of the bagasse feeder motors into the furnace ( $\Delta u(t)$ ) as the input variable. The fundamental disturbance ( $D(t)$ ) that

affects this process is the % of moisture content in the bagasse that enters the furnace [10].

The mathematical model of the steam pressure in the steam drum of the bagasse-fired boiler under study is obtained by employing a system identification procedure based on the step response [48], [49]. The identification experiment initially lowers the steam pressure in the steam drum of the boiler to a value that does not affect the turbine operation (22 kgf/cm<sup>2</sup>) and then carries this variable to its nominal operating value (23.5 kgf/cm<sup>2</sup>) through the use of a step input signal. The mathematical model of the steam pressure that is obtained will, therefore, represent the nominal dynamic behavior of this variable (nominal plant).

The speed of the bagasse feeder motor receives an increment  $\Delta u(t)$  of 10%. The data concerning the steam pressure variation ( $\Delta y(t)$ ), along with those regarding the increase in the speed of the bagasse feeder motors ( $\Delta u(t)$ ) are registered and stored in a computer. The experimental response of the nominal process to that step command is shown in Fig. 2.

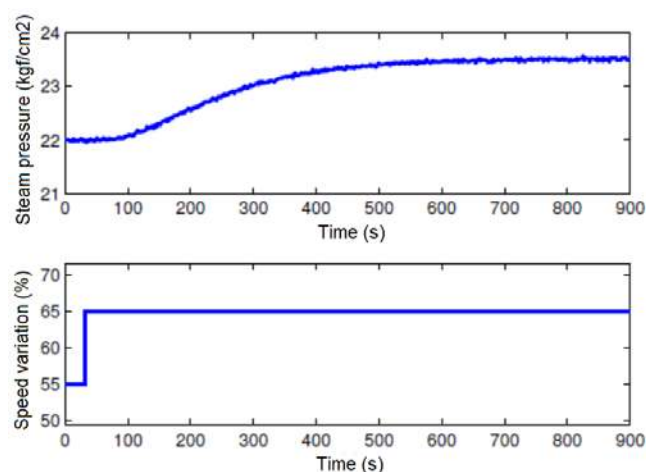


**FIGURE 2.** Experimental response to a step command of the nominal process.

This dynamics can be represented by employing a third-order overdamped system with a time delay:

$$a_3 \cdot \frac{d\Delta y^3}{dt^3} + a_2 \cdot \frac{d\Delta y^2}{dt^2} + a_1 \cdot \frac{d\Delta y}{dt} + a_0 \cdot \Delta y(t) = K \cdot \Delta u(t - \tau) \quad (1)$$

where  $a_i$  ( $i = 0, \dots, 3$ ) are real constant coefficients,  $K$  is the static gain and  $\tau$  the time delay.

The transfer function of this system is:

$$G(s) = \frac{\Delta y(s)}{\Delta u(s)} = \frac{K \cdot e^{-\tau \cdot s}}{(T_1 s + 1)(T_2 s + 1)(T_3 s + 1)} \quad (2)$$

where  $T_1$ ,  $T_2$ , and  $T_3$  are the time constants.

The nominal model is denoted as  $G_0(s)$  and its parameters, which are estimated using the identification procedure, are  $K_0 = 0.36$  kgf/cm<sup>2</sup>,  $T_{10} = 81.2$  s,  $T_{20} = 62.7$  s,  $T_{30} = 34.1$  s, and  $\tau_0 = 50$  s.

The validation of linear model (2) with the estimated nominal parameters is shown in Fig. 3. This figure shows a good agreement between the experimental response to a step and the prediction provided by our nominal mathematical model.

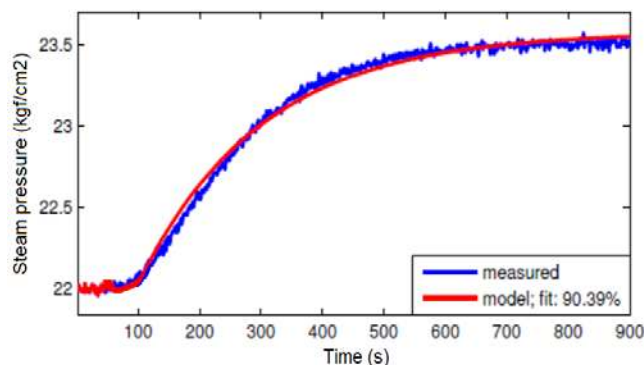


**FIGURE 3.** Validation of linear model (2) with the estimated values of the nominal parameters.

The most important property of fuels is their calorific value, which is defined as the amount of heat  $Q(t)$  produced by the complete combustion of fuel measured in units of energy per amount of material [38]. In the case of bagasse, the calorific value depends mainly on the % of its contents of moisture and cane fiber (cellulose) [1].

The calorific value of bagasse is 19250 kJ/kg at 0% moisture and 9950 kJ/kg at 48% moisture [7], [11]. The percentage of moisture content of the bagasse is, therefore, the most significant parameter by which to determine its calorific value, signifying that the higher the moisture content, the lower the calorific value of the bagasse [7]. A good milling process will result in a low bagasse moisture content, while an increase in the fiber content of the sugar cane increases the fiber content of the bagasse, which implies an increase in the calorific value.

During sugar harvesting, and as result of a complex agro-industrial process of sugarcane transformation, the moisture and fiber contents in the bagasse undergo wide variations. They produce changes in the calorific value  $Q(t)$  of the bagasse in an operation range  $[Q_{\min}, Q_{\max}]$  [4], [40], which affect the dynamic behavior of the steam pressure in the steam drum of the boiler.

After developing more real-time experiments in the steam pressure of our bagasse-fired boiler, and using a robust system identification procedure, e.g., [45], it was shown that variations in the bagasse calorific value in the operation range  $[Q_{\min}, Q_{\max}]$  cause variations in the static gain of the mathematical model (2) in a range  $[K_{\min}, K_{\max}]$ , which is defined by:

$$0.1 \leq K \leq 1.12 \quad (3)$$

Any controller of the steam pressure in the steam drum of the boiler under study must, therefore, guarantee, a priori, a minimum performance in the whole range of variation of the dynamic parameters (model uncertainties) of the mathematical model (2).

Furthermore, the plant undergoes the effect of non-measurable disturbances. This effect has been modelled as a step input,  $z(t)$ , that passes through a first order filter:

$$W(s) = \frac{1}{T_4 s + 1} \quad (3)$$

which has a time constant  $T_4 = 17.5$  s.

Fig. 4 represents the complete model. In order to simplify the notation, the incremental variables  $\Delta u$  and  $\Delta y$  have been replaced with  $u$  and  $y$ .

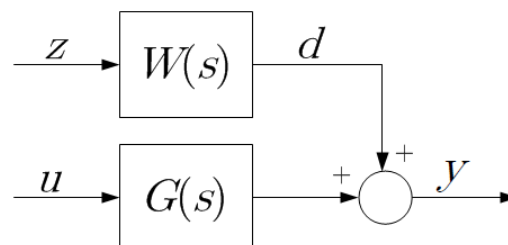


**FIGURE 4.** Block diagram of the linear model.

### III. FRACTIONAL ORDER CONTROLLER DESIGN

#### A. CONTROL OBJECTIVES

When the calorific value of the bagasse changes, the static gain of our process varies in the wide range (3). Taking into account this gain variation, the control objectives are the following:

1. Zero steady state error,  $e_{ss} = 0$ , to a step command.
2. A small overshoot,  $M_p = 5\%$ , of the closed-loop nominal process.
3. A settling time of the closed-loop nominal process that should be about twice the value of the open-loop settling time. Since the open loop settling time is  $t_s^{op} = 427$  s, a value of  $t_s = 824$  s is chosen for the nominal closed-loop settling time.
4. A good performance of the closed-loop process when the static gain takes values in its entire range (3). In this respect, the quality of the closed-loop behavior is evaluated by means of the steam pressure uniformity, which can be assessed by employing the Integral Absolute Error [50]:

$$IAE = \int_0^{\infty} |y^*(t) - y(t)| dt \quad (5)$$



where  $y^*$  is the steam pressure reference and  $y$  is the actual steam pressure.

Other desired control objectives that are usual in this kind of processes are:

5. Good disturbance rejection in all cases: with the nominal process and when the gain changes.
6. Low sensitivity to noise in the measurement.
7. Low sensitivity to the sampling time.

These control objectives are desirable and can also be evaluated by means of the steam pressure uniformity (IAE index).

## B. CONTROL SCHEME AND CONTROLLERS

Let us assume the standard feedback control scheme shown in Fig. 5, in which  $y^*$  is the steam pressure reference,  $e$  is the error signal,  $u$  is the control signal,  $y$  is the boiler steam pressure and  $z$  is a step signal that passes through the filter  $W(s)$ , yielding the disturbance  $d$ . Furthermore,  $C(s)$  and  $G(s)$  are the transfer functions of the controller and the process (2), respectively.

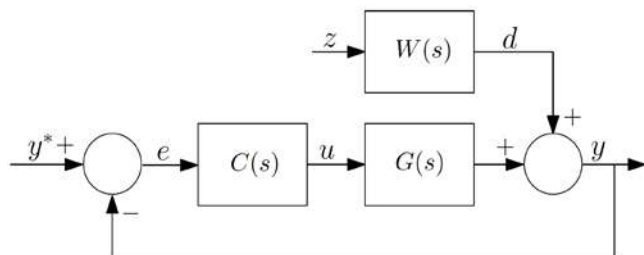


FIGURE 5. Block diagram of the proposed control scheme.

Some previous research has proved that fractional-order controllers may increase the robustness of closed-loop processes that have a time delay [27], [35]. This work, therefore, explores the advantages of using fractional-order controllers in our process. The performances of our fractional-order controller and conventional  $PI$  and  $PID$  controllers will now be compared.

A  $PID$  controller is of the form [50]:

$$C_{PID}(s) = K_p + \frac{K_i}{s} + K_d s \quad (6)$$

where  $K_p$ ,  $K_i$  and  $K_d$  are the proportional, integral and derivative gains, respectively. A  $PI$  controller is a particular example of the previous case in which  $K_d = 0$  is made:

$$C_{PI}(s) = K_p + \frac{K_i}{s} \quad (7)$$

The proposed fractional-order controller is a  $PI$  controller in which the integral operator has been substituted for a fractional-order integral operator [27]. This controller is known as the  $PI^\alpha$  controller and will, hereafter in this paper, also be denoted as the  $FPI$  controller. It has the

form [25]:

$$C_{FPI}(s) = K_p + \frac{K_i}{s^\alpha} \quad (8)$$

where  $\alpha$  is the non-integer order of the integral action and the gains have the same meaning as in the  $PI$  and  $PID$  controllers.

Note that controllers (6)–(8) fulfill the first control objective because all of them have an integral action (of integer or fractional order) that yields zero steady state error when a step command is applied.  $PI$  controllers have two parameters that must be tuned, while  $PID$  and  $PI^\alpha$  controllers have three.

Two parameters of all these controllers can be tuned to fulfill the nominal requirements  $M_p = 5\%$ , and  $t_s = 824$  s (second and third control objectives).

The third parameter of the  $PID$  and  $PI^\alpha$  controllers can be tuned in order to improve the closed-loop performance when the static gain changes in the range (3) (fourth control objective).

## C. TUNING PROCEDURE

Frequency techniques are used to tune controller gains, assuming that the overshoot is related to the phase margin,  $\phi_m$ , and the settling time to the gain crossover frequency,  $\omega_c$ . This tuning procedure is commonly used in process control [26], [27], [37].

The closed-loop transfer function between  $y^*$  and  $y$  of the scheme shown in Fig. 5 is:

$$M(s) = \frac{C(s)G(s)}{1 + C(s)G(s)} \quad (9)$$

and its corresponding open-loop transfer function is:

$$L(s) = C(s)G(s) \quad (10)$$

Provided that the pair of desired frequency specifications are  $\phi_m$  and  $\omega_c$  for the nominal process, the following complex equation can be used to tune the gains of the controllers [35]:

$$L(j\omega_c) = -e^{j\phi_m} \quad (11)$$

Upon replacing  $C(s)$  with equations (6), (7), and (8) in (10) and (11), the following tuning equations are easily obtained:

$$PI \text{ controller: } \begin{cases} K_p = \Re(\xi) \\ -\omega_c \Im(\xi) \end{cases} \quad (12)$$

$$PID \text{ controller: } \begin{cases} K_p = \Re(\xi) \\ K_i = \omega_c^2 K_d - \omega_c \Im(\xi) \end{cases} \quad (13)$$

$$PI^\alpha \text{ controller: } \begin{cases} K_p(\alpha) = \Re(\xi) + \frac{\Im(\xi)}{\tan\left(\frac{\pi\alpha}{2}\right)} \\ K_i(\alpha) = -\frac{\omega_c^\alpha \Im(\xi)}{\sin\left(\frac{\pi\alpha}{2}\right)} \end{cases} \quad (14)$$

where

$$\xi = \frac{-e^{-j\phi_m}}{G_0(j\omega_c)} \quad \text{and } \Re() \text{ and } \Im() \text{ are the real and imaginary components of a complex number, respectively.}$$

Gains  $K_p$ , and  $K_i$  of a  $PI$  controller are defined in their totality by employing the two specifications  $\phi_m$  and  $\omega_c$  (see (12)). However, the gain  $K_i$  of a  $PID$  controller depends on the gain  $K_d$  (see (13)), which can be freely chosen, and the two gains of the  $PI^\alpha$  controller depend on the non-integer integral action,  $\alpha$  (see (14)), which can also be freely chosen. This signifies that  $K_d$ , in the case of the  $PID$  controller, and  $\alpha$ , in the case of the  $PI^\alpha$  controller, will be chosen to satisfy the fourth control objective: obtaining a good closed loop performance for all the values of  $K$  comprised in the range (3). Since stability robustness to gain changes is assessed by the gain margin (e.g. [50]), we propose to achieve the fourth objective by choosing the parameters  $K_d$  and  $\alpha$ , which maximize the gain margin.

#### IV. SIMULATED RESULTS AND DISCUSSION

The simulations were carried out using MATLAB with a sampling period of  $T = 0.2$  s. The fractional-order action of the controllers was implemented by employing the Grünwald-Letnikov algorithm (without any series truncation) in order to obtain accurate results [27]:

$${}_a D_t^\beta f(t) = \lim_{t \rightarrow 0} T^{-\beta} \sum_{j=0}^{\left\lfloor \frac{t-a}{T} \right\rfloor} (-1)^j \binom{\beta}{j} f(t-jT) \quad (15)$$

In this expression,  $\beta \in \mathbb{R}$  is the fractional-order operator that signifies a fractional derivative if  $\beta > 0$  and a fractional integral if  $\beta < 0$  of the function  $f(t)$ ,  $[\cdot]$  represents the integer part, and the combinatorial function has been generalized in the following respect:

$$\binom{\beta}{l} = \frac{\beta(\beta-1)\dots(\beta-l+1)}{l!} \quad (16)$$

Expressions (15), (16) are used to implement the fractional-order integral term of the  $PI^\alpha$  controller by simply making  $\beta = -\alpha$ .

We verified that (15) yields an accurate approximation of the operator  $1/s^\alpha$  if the above sampling period is used.

Coefficients (16) were determined prior to the simulation.

#### A. CONTROLLERS FOR THE NOMINAL PROCESS

**PI controller:** Specifications  $M_p = 5\%$  and  $t_s = 824.2$  s are achieved by employing a single pair of parameters ( $K_p$ ,  $K_i$ ) of a  $PI$  controller. Since analytical expressions that relate the closed-loop time specifications ( $M_p$ ,  $t_s$ ) to the frequency specifications ( $\phi_m$ ,  $\omega_c$ ) are not available for third order plus time delay transfer functions combined with  $PI$  controllers, the gains ( $K_p$ ,  $K_i$ ) have to be determined numerically using a search method. A procedure composed of the following steps has been used for this purpose:

- 1) The analytical relations existing between the pairs of specifications ( $M_p$ ,  $t_s$ ) and ( $\phi_m$ ,  $\omega_c$ ) in the case of simple second order systems, e.g. [50], are used to obtain initial values ( $\phi_{m,0}$ ,  $\omega_{c,0}$ );
- 2) Values ( $\phi_{m,0}$ ,  $\omega_{c,0}$ ) are introduced into expressions (12) in order to yield the initial values of the gains ( $K_{p,0}$ ,  $K_{i,0}$ );
- 3) A search procedure is carried out in which specifications ( $\phi_m$ ,  $\omega_c$ ) are modified. Consider the step  $i$ :
  - a) For each pair ( $\phi_{m,i}$ ,  $\omega_{c,i}$ ), gains ( $K_{p,i}$ ,  $K_{i,i}$ ) are calculated using (12).
  - b) The step response of the closed-loop system using the  $PI$  controller with gains ( $K_{p,i}$ ,  $K_{i,i}$ ) is simulated and the corresponding specifications ( $M_{p,i}$ ,  $t_{s,i}$ ) are obtained.
  - c) The performance index  $\chi_i = |M_{p,i} - M_p| + |t_{s,i} - t_s|$  is calculated.
  - d) The search finishes if  $\chi_i < \chi$ , where  $\chi$  is the maximum error allowed in the pair of specifications. If  $\chi_i > \chi$ , a new pair ( $\phi_{m,i+1}$ ,  $\omega_{c,i+1}$ ) is determined in the descending direction of the cost  $\chi_i$  at the point ( $\phi_{m,i}$ ,  $\omega_{c,i}$ ). Details of this procedure can be found in [32].

Taking into account that  $M_p = 5\%$  approximately corresponds to  $\phi_m = 65^\circ$  (see [27]) and that  $\omega_c \approx \pi/t_s$ , the initial estimation of the frequency specifications is  $\omega_{c,0} = 0.0038$  rad/s and  $\phi_{m,0} = 65^\circ$ . The frequency specifications that exactly guarantee the nominal time specifications are subsequently adjusted by following the above procedure. They are  $\omega_c = 0.002113$  rad/s and  $\phi_m = 61.68^\circ$ . Tuning equations (12) with these values then yield the controller:

$$C_{PI} = -0.3359 + \frac{0.005861}{s} \quad (17)$$

Fig. 6 plots the time response yielded by the nominal process when using this controller.

**PID controller:** Once the parameter  $K_d$  has been chosen, parameters  $K_p$  and  $K_i$  are calculated from this value and the frequency specifications  $\phi_m$  and  $\omega_c$  by using (13). In this case, a set of  $PID$  controllers that depend on the parameter  $K_d$  can be obtained that fulfill the nominal time specifications. It is well-known that if  $\phi_m$  and  $\omega_c$  remain

constant but  $K_d$  changes, the time responses do not maintain the same  $M_p$  and  $t_s$  values [33]. The application of tuning equation (13) does not, therefore, guarantee the desired nominal specifications  $M_p$  and  $t_s$ .

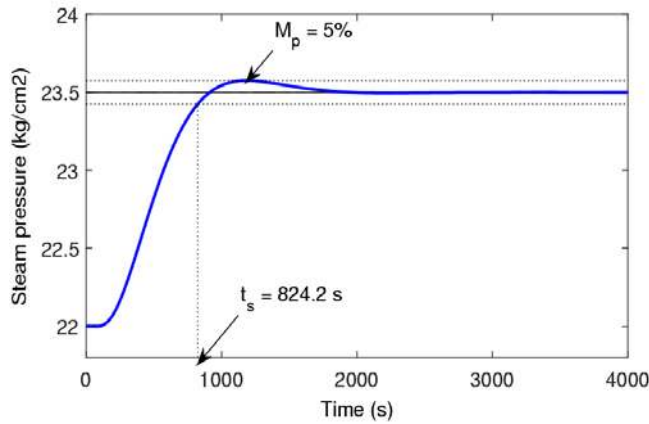


FIGURE 6. PI controller: nominal time response.

For a given value of  $K_d$ , and using the frequency requirements of the  $PI$  controller obtained in the previous subsection,  $\phi_m = 61.68^\circ$  and  $\omega_c = 0.002113$  rad/s, the application of the procedure described in Subsection  $PI$  controller (in which now expressions (13) are applied instead of (12) and the  $PID$  controllers are simulated instead of  $PI$  s) yields the  $PID$  controller that verifies the nominal time specifications required. This procedure can be repeated for a set of  $K_d$  values, yielding a set of  $PID$  controllers that exactly yield the nominal time specifications required. The two sets of gains obtained are fitted by employing third order polynomials:

$$\begin{aligned} K_p &= -4.614 \times 10^{-10} K_d^3 - 1.259 \times 10^{-6} K_d^2 \\ &\quad + 0.003556 K_d - 0.03256 \\ K_i &= -2.797 \times 10^{-12} K_d^3 - 3.201 \times 10^{-9} K_d^2 \\ &\quad + 1.066 \times 10^{-5} K_d + 0.005852 \end{aligned} \quad (18)$$

for  $K_{d1} \in [-112, 403]$

The norms of the residual values of these fittings are 0.003669 for  $K_p(K_d)$  and 0.00003199 for  $K_i(K_d)$ , which are regarded as very low. Functions (18), therefore, accurately represent the locus in the controller parametric space that simultaneously achieves  $M_p$  and  $t_s$  specifications.

Controllers (18) provide nominal closed-loop responses with time specifications that are very close to those required. The maximum error of  $M_p$  is 0.8% and that of  $t_s$  is 0.25%. Fig. 7a shows the step responses yielded by the  $PID$  controllers (18) in the case of the nominal process. Fig. 7b shows the step responses yielded by the  $PID$  controllers tuned using expression (13) with  $\omega_c = 0.002113$  rad/s and  $\phi_m = 61.68^\circ$ . Large variations of  $M_p$  and  $t_s$  are

produced in this last case (the settling time changes from 820 s to 2150 s approximately). The time responses shown in Fig. 7 sometimes exhibit oscillatory behavior when they begin, which is caused by the derivative term of the controllers.

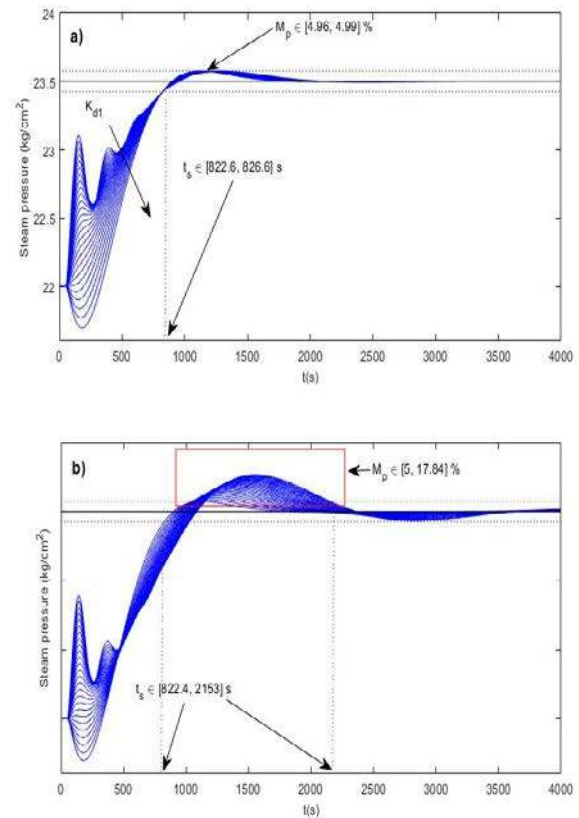


FIGURE 7. PID set: nominal time responses using: a) the time domain tuning method and b) the frequency domain tuning method with expression (13).

$PI^\alpha$  controller: The parameters  $K_p$  and  $K_i$  of this controller can be obtained from tuning equations (14), provided that the two frequency specifications are  $\phi_m$  and  $\omega_c$ , and that the fractional order is  $\alpha$ . This last parameter can be freely chosen and will be used in the following section to improve the robustness of the closed-loop system to process gain changes. In accordance with (14), a set of controllers will be defined depending on the values of  $\alpha$  in a specified range. As explained in [34], if  $\phi_m$  and  $\omega_c$  remain constant while  $\alpha$  changes, the resulting time responses have the values  $M_p$  and  $t_s$ , which vary and are different from the desired specifications. This signifies that equation (14) cannot be applied in order to tune the proposed  $PI^\alpha$  controllers because the controllers yielded do not provide the nominal time response required.

For a given value of  $\alpha$ , and again using the frequency requirements of the  $PI$  controller obtained in Subsection  $PI$  controller,  $\omega_c = 0.002113$  rad/s and  $\phi_m = 61.68^\circ$ , the

application of the procedure shown in Subsection  $PI$  controller (in which expressions (14) are now applied instead of (12) and the  $PI^\alpha$  controllers obtained are simulated instead of  $PI$  s) yields the  $PI^\alpha$  controller that verifies the nominal time specifications. This procedure can be repeated for a set of  $\alpha$  values, yielding a set of  $PI^\alpha$  controllers that exactly yield the nominal time specifications required. The two sets of gains obtained are fitted by third order polynomials:

$$\begin{aligned} K_p &= 179.6\alpha^3 - 519.8\alpha^2 + 506.2\alpha - 166.1 \\ K_i &= -0.1664\alpha^3 + 0.6269\alpha^2 - 0.7887\alpha + 0.3341 \end{aligned} \quad (19)$$

for  $\alpha \in [0.92, 1.15]$

The norms of the residual values of these fittings are 0.01554 for  $K_p(\alpha)$  and 0.000011627 for  $K_i(\alpha)$ , which are regarded as very low. Functions (19), therefore, accurately represent the locus in the controller parametric space that simultaneously achieves  $M_p$  and  $t_s$  specifications.

Controllers (19) provide nominal time responses with time specifications that are very close to those required. The maximum error of  $M_p$  is 2.2% and that of  $t_s$  is 0.6%. Fig. 8a shows the nominal step responses yielded by (19) and Fig. 8b the responses yielded by the controllers designed using the frequency domain method with  $\omega_c = 0.002113$  rad/s and  $\phi_m = 61.68^\circ$  (without subsequently carrying out the fine tuning provided by the time domain method). Large variations of  $M_p$  and  $t_s$  can be observed in this last figure (the settling time changes from 824 s to 2250 s approximately).

Moreover, a comparison between Figs 7a and 8a shows that  $PI^\alpha$  controllers provide a much better time response uniformity than that of  $PID$  controllers (e.g., the initial oscillations of the  $PID$  responses are prevented).

### B. OPTIMAL CONTROLLERS FOR GAIN VARIATION

The robustness to changes in the process gain  $K$  is improved in this subsection. The most robust controllers of the  $PID$  set (18) and the  $PI^\alpha$  set (19) are determined. The transfer functions of the sets of  $PID$  and  $PI^\alpha$  controllers are obtained by replacing (18) in (6) and (19) in (8), respectively. They are respectively represented by  $C_{PID}(s)$  and  $C_{FPI}(s)$ , and depend on the parameters  $K_d$  and  $\alpha$ , respectively. The open-loop transfer functions are obtained by substituting  $C_{PID}(s)$  and  $C_{FPI}(s)$  in (10). The open-loop transfer functions when using  $PID$  controllers are represented by  $L_{PID}(s, K_d)$ , and when using  $PI^\alpha$  controllers by  $L_{FPI}(s, \alpha)$ . In both expressions, the dependence of the controllers on parameters  $K_d$  and  $\alpha$  has been made explicit. The phase crossover frequency of  $L_{PID}(j\omega, K_d)$  is denoted as  $\omega_{PID}(K_d)$  and its gain margin as  $M_{PID}(K_d)$ . The phase crossover frequency of

$L_{FPI}(j\omega, \alpha)$  is denoted as  $\omega_{FPI}(\alpha)$  and its gain margin as  $M_{FPI}(\alpha)$ . Fig. 9 plots functions  $M_{PID}(K_d)$  and  $M_{FPI}(\alpha)$ . The maxima of these functions are denoted as  $M_{PID}^*$  and  $M_{FPI}^*$ , respectively. Fig. 9 shows that these maxima are higher than the gain margin of the  $PI$  controller, which is  $M_{PI} = 4.214$ .

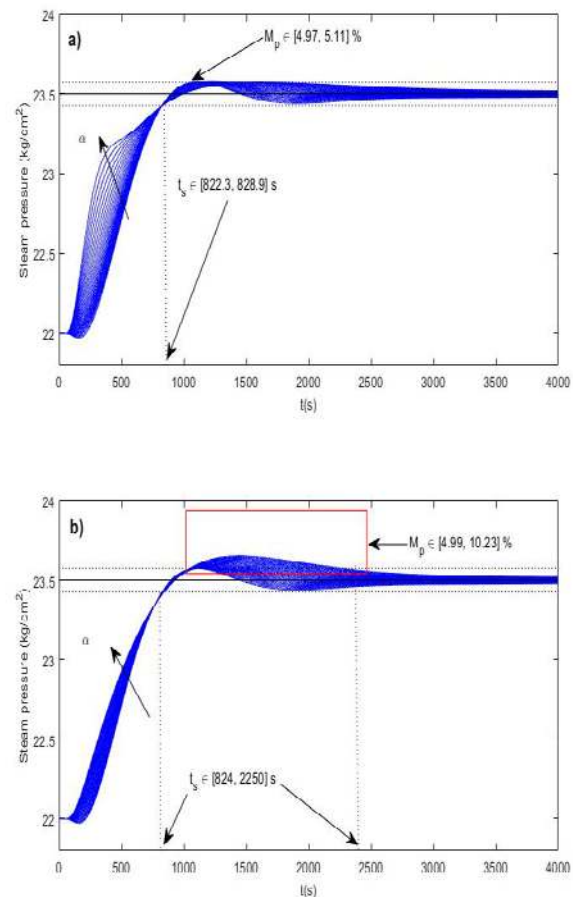


FIGURE 8.  $PI^\alpha$  set: nominal time response: a) time domain tuning method; b) frequency domain tuning method.

The optimal  $PID$  controller is obtained for  $K_d = 50$ :

$$C_{PID}^*(s) = 0.14203 + \frac{0.0063769}{s} + 50s \quad (20)$$

which provides a gain margin  $M_{PID}^* = 17.25$ .

The optimal  $PI^\alpha$  controller is obtained for  $\alpha = 1.076$ :

$$C_{FPI}^*(s) = 0.55963 + \frac{0.0039729}{s^{1.076}} \quad (21)$$

which provides a gain margin  $M_{FPI}^* = 7.379$



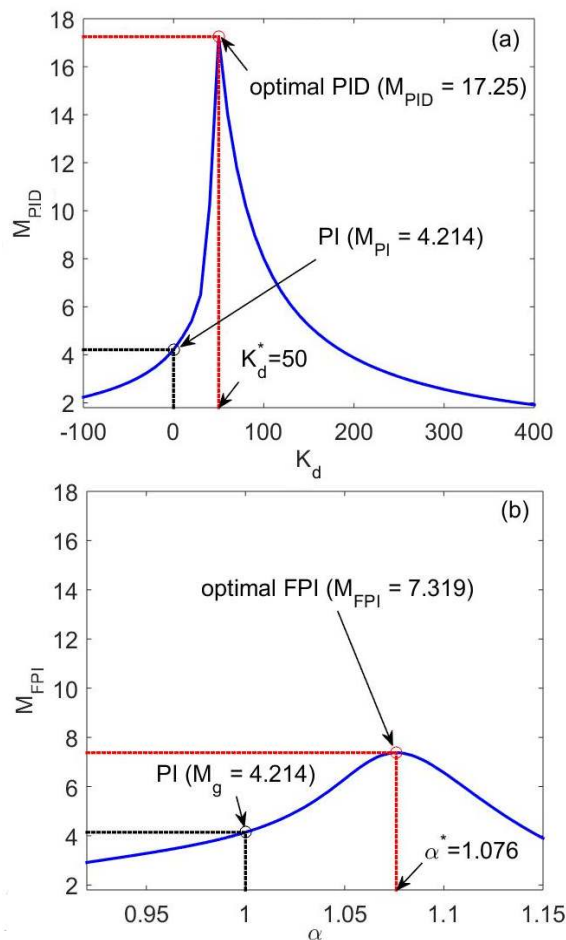


**FIGURE 9.** Selection of the optimal PID and  $PI^\alpha$  controllers: a)  $M_{PID}(K_d)$ ; b)  $M_{FPI}(\alpha)$ .

### C. PERFORMANCE WHEN THE GAIN CHANGES

Fig. 10 shows the behavior of the controlled system when the process gain changes in the range (3). Fig. 10a plots the step responses using the  $PI$  controller (17), Fig. 10b using the  $PID$  controller (20) and Figure 10c using the  $PI^\alpha$  controller (21).

As shown in Fig. 10, the optimal  $PI^\alpha$  controller provides a better uniformity response than the optimal  $PID$  and the  $PI$  controllers, although the  $PID$  optimal controller achieves the highest gain margin (see Fig. 9a).

The curves of the indexes  $IAE$  (5) obtained using the  $PI$ , optimal  $PID$  and optimal  $PI^\alpha$  controllers when the plant gain changes in the range (3) are plotted in Fig. 11 in order to quantify the improvement to uniformity provided by the  $PI^\alpha$  controller. This figure shows that the optimal  $PI^\alpha$  controller behaves better than the  $PI$  and the optimal  $PID$  controllers. For low values of the gain, the  $PI^\alpha$  and  $PID$  controllers yield similar results but, when the gain  $K$  increases, the  $PI^\alpha$  controller behaves much better, since it decreases the  $IAE$  index as  $K$  increases. For  $K = 1.12$  (maximum value allowed for the gain), the  $PI^\alpha$  controller reduces the  $IAE$  index to 29.75% of the nominal value.

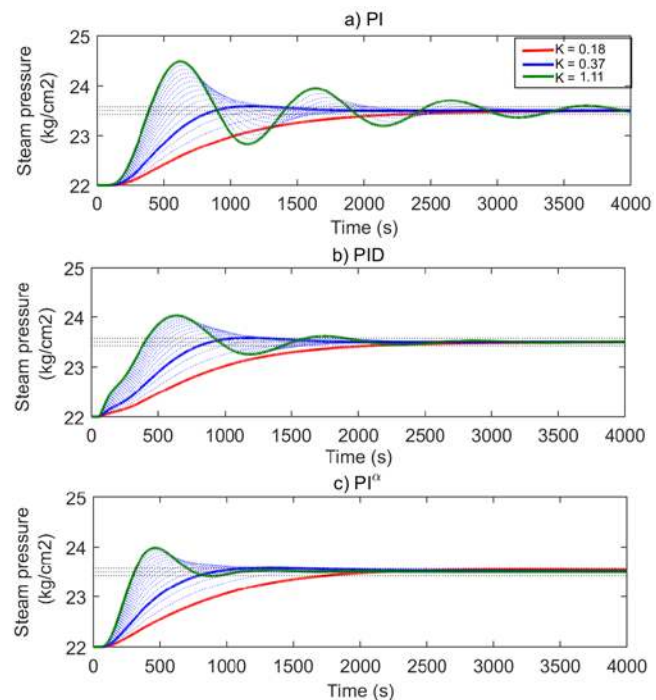


**FIGURE 10.** Time response for  $K \in [0.17, 1.12]$ : a)  $PI$  (17); b) optimal  $PID$  (20), and c) optimal  $PI^\alpha$  (21).

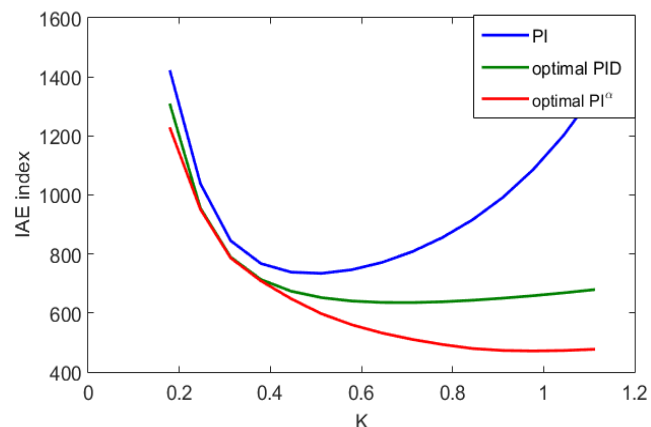


**FIGURE 11.** IAE index for  $K \in [0.17, 1.12]$ : a)  $PI$  (17); b) optimal  $PID$  (20), and c) optimal  $PI^\alpha$  (21).

The  $PI$ , the optimum  $PID$  and the optimum  $PI^\alpha$  controllers, therefore, provide the time specifications required for the nominal process ( $e_{ss} = 0$ ,  $M_p = 5\%$  and  $t_s = 824.2$  s), which are control objectives 1, 2 and 3. However, the uniformity of the steam pressure achieved by the  $PI^\alpha$  controller when the gain changes in the range (3) significantly outperforms those achieved by the  $PI$  and  $PID$  controllers, which is control objective 4.

### D. DISTURBANCE REJECTION BEHAVIOR

This subsection assesses the ability of the  $PI$ ,  $PID$  and  $PI^\alpha$  controllers to reject disturbances, even when the gain changes in the range (3).

Fig. 12 compares the time responses provided by the  $PI$ ,  $PID$  and  $PI^\alpha$  controllers in the cases of the nominal process and when  $K$  changes in the range (3). Fig. 13 plots the  $IAE$  indexes provided by these three controllers when  $K$  varies.

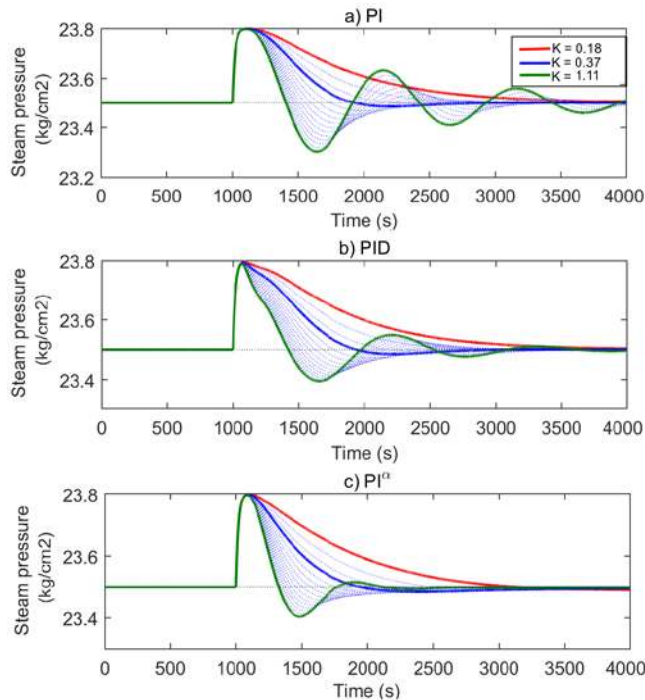


**FIGURE 12.** Disturbance rejection for  $K \in [0.17, 1.12]$ : a)  $PI$  (17); b) optimal  $PID$  (20), and c) optimal  $PI^\alpha$  (21).

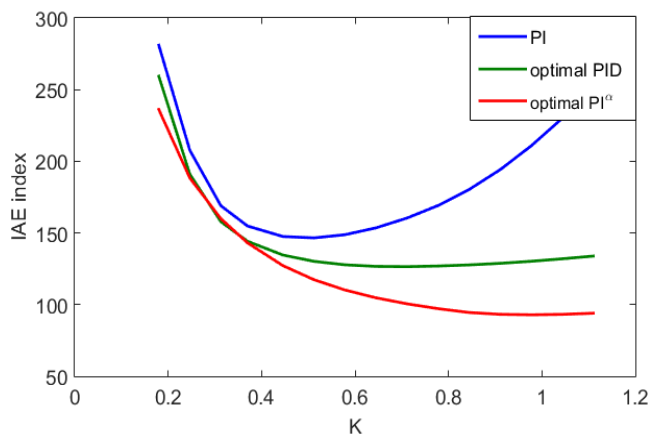


**FIGURE 13.** Disturbance rejection:  $IAE$  indexes for  $K \in [0.17, 1.12]$ : a)  $PI$  (17); b) optimal  $PID$  (20), and c) optimal  $PI^\alpha$  (21).

These results show that the  $PI^\alpha$  optimal controller also improves the steam pressure uniformity in the presence of non-measurable disturbances. As in the case of set point changes, the  $PI^\alpha$  and  $PID$  controllers provide similar results for low values of the gain, but when the gain increases, the  $PI^\alpha$  controller yields lower  $IAE$  values than the  $PID$  controller, thus increasing the steam pressure

uniformity.

### E. ANOTHER PLANT PARAMETER VARIATION

This subsection compares the performance of the three controllers when  $T_1, T_2, T_3$ , or  $\tau$  change slightly, in order to check their fragility. Let us assume that these parameters change  $\pm 10\%$  with regard to their nominal values. The worst case is when the three time constants take their lowest values and the time delay takes its highest value. This case corresponds to  $T_1 = 72.36$  s,  $T_2 = 57.42$  s,  $T_3 = 31.68$  s and  $\tau = 55$  s. Fig. 14 plots the  $IAE$  index when the gain changes and the other parameters take the previous values.

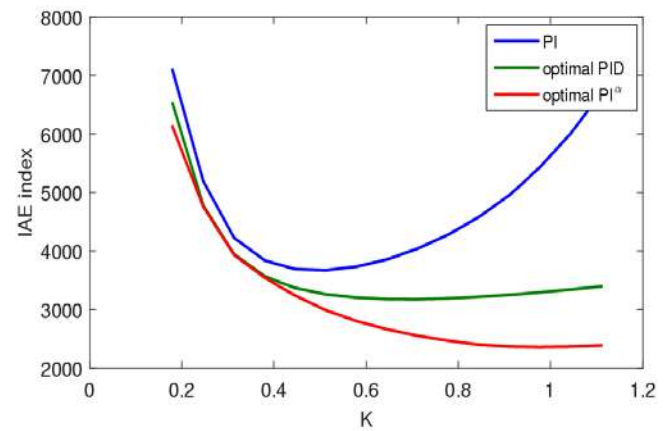


**FIGURE 14.** Another plant parameter variation:  $IAE$  index for  $K \in [0.17, 1.12]$ : a)  $PI$  (17); b) optimal  $PID$  (20), and c) optimal  $PI^\alpha$  (21).

These results are similar to those obtained in the previous cases: the  $PID$  and  $PI^\alpha$  controllers have similar behavior for low values of the gain, but the  $PI^\alpha$  controller improves the steam pressure uniformity at medium and high values of the process gain.

### E. NOISE SENSITIVITY AND SAMPLE TIME SENSITIVITY

In this subsection, the steam pressure uniformities of the three controllers are compared in the presence of noise and when the sampling period increases. Fig. 15 plots the  $IAE$  index obtained in the case of adding a noise with a uniform distribution of amplitude 0.02 to the output  $y(t)$  and simultaneously using a sampling period 100 times higher than that used in the previous simulations ( $T = 20$  s). This figure shows that the results are quite similar to those obtained in the previous sections and that the  $PI^\alpha$  controller improves the steam pressure uniformity with regard to the  $PI$  and  $PID$  controllers when the gain increases.

## V. CONCLUSION

This paper studies the closed-loop control of the steam pressure in the steam drum of a bagasse-fired boiler. First, an identification process has been carried out that yields a

linear third order plus time delay transfer function of the incremental model of the nominal process. An output disturbance has also been characterized as the output of a first order filter whose input is a step signal. Moreover, a large range of variation in the static gain has been characterized.

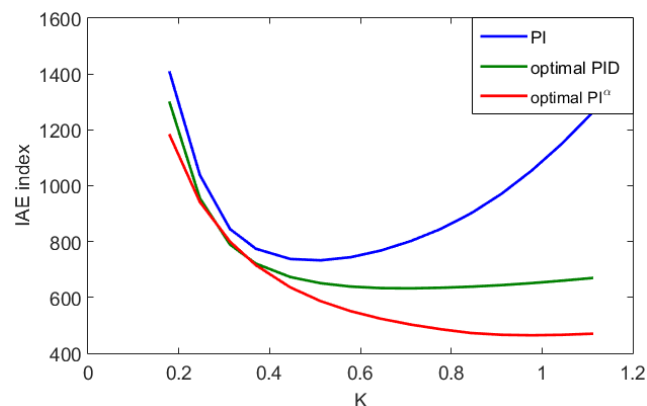


FIGURE 15. Noise and sample time sensitivity: IAE indexes for  $K \in [0.17, 1.12]$ : a)  $PI$  (17); b) optimal  $PID$  (20), and c) optimal  $PI^\alpha$  (21).

The design of  $PID$  and  $PI^\alpha$  controllers that are robust to gain changes has also been detailed. The design procedure comprises two stages: 1) the sets of  $PID$  controllers and  $PI^\alpha$  controllers that provide the desired overshoot and settling time for the nominal process, along with zero steady state error to setpoint changes, are determined by employing a search procedure; 2) the controllers of each of these two sets that maximize the gain margin are chosen. The objective of this second stage is to choose controllers that significantly improve the robustness to the large gain changes experimentally observed (the maximum process gain is about 7 times the minimum gain).

The robustness of the controllers designed has been assessed by using the well-known  $IAE$  index and calculating its values in the entire gain range. The performances as regards set point changes, modelled disturbances, parametric variations of the time constants and the time delay, output noise and sampling period variations have been studied. The analysis carried out has yielded that: a) the optimum  $PID$  and  $PI^\alpha$  controllers significantly outperform the  $PI$  controller, and b) the optimum  $PI^\alpha$  significantly outperforms the optimum  $PID$ , especially in the high gain zone.

Since a  $PI$  controller has two parameters that must be tuned, while the  $PID$  and  $PI^\alpha$  controllers have three, it is to be supposed that the optimum  $PID$  and  $PI^\alpha$  controllers will outperform the robustness of the  $PI$  controller. What is remarkable is the improvement as regards robustness achieved when using the  $PI^\alpha$  rather than the  $PID$  controller. Since both controllers have three parameters that must be tuned (they have an equivalent complexity from the design point of view), the improvement cannot be attributed to an increase in the complexity of one of the controllers,

i.e., to the fact that a higher number of parameters would be available to be tuned, but rather to the structure of the fractional-order controller, that appears to be better than the structure of the  $PID$  controller as regards boosting the robustness to the static gain changes of our process.

The next objective of our research is the practical implementation of the  $PI^\alpha$  controller designed in the bagasse-fired boilers of the '30 de Noviembre' sugarcane industry using a PLC SIMATIC S7-300.

The benefits obtained thanks to the increase in the robustness and effectiveness of the control of the steam pressure in the steam drum of the boiler are immediately translated into an increase in energy efficiency and greater environmental protection, which are attained by reducing the load of gases and pollutant particles.

Finally, it is worth mentioning that, although the conclusions presented in this paper are concerned only with our particular industrial process, the controller design method and the procedures outlined can also be applied to other processes with different types of transfer functions.

## REFERENCES

- [1] O. Sahu, "Assessment of sugarcane industry: suitability for production, consumption, and utilization," *Ann. Agrar. Sci.*, vol. 16, pp. 389–395, Jul. 2018.
- [2] A.K. Chandel, S.S. da Silva, W. Carvalho, and O.V. Singh, "Sugarcane bagasse and leaves: foreseeable biomass of biofuel and bio-products," *J. Chem. Technol. Biotechnol.*, vol. 87, no. 1, pp. 11–20, Jan. 2012.
- [3] E. Hugott, "Handbook of cane sugar engineering," México: Editorial Continental S.A., 1996.
- [4] P. Rein, "Cane sugar engineering," Berlin, Germany: Ed. Bartens, 2007.
- [5] C. de Prada Moraga, E. Baeyens Lazaro, and R. Rivas-Perez, "Introduction to the special section of the modelling, control and optimization of the sugar industry," *Rev. Iberoam. Autom. Inf. Ind.*, vol. 6, no. 3, pp. 5–9, Jun. 2009.
- [6] J. Barroso, F. Barreras, H. Amaveda, and A. Lozano A., "On the optimization of boiler efficiency using bagasse as fuel," *Fuel*, vol. 82, no. 12, pp. 1451–1463, 2003.
- [7] A. Alena, and O. Sahu, "Cogenerations of energy from sugar factory bagasse," *J. Energy Eng.*, vol. 1, no. 2, pp. 22–29, 2013.
- [8] R. Rivas-Perez, "Generadores de vapor de bagazo y su control," in *Libro Blanco del Control Automático en la Industria de la Caña de Azúcar*, Diazzo Plotter Suministros, Programa CYTED, Red de Automatización y Control de la Industria de Transformación de la Caña de Azúcar, España, 195–230, 2011.
- [9] S. G. Dukelow, "The control of boilers," second edition, North Carolina, NC, USA: Instrument Society of America, 1991.
- [10] R. Rivas-Perez, F. Castillo-García, J. Sotomayor-Moriano J., and V. Feliu-Batlle, "Robust fractional order control of steam pressure in steam drum of bagasse boiler," *Rev. Iberoam. Autom. Inf. Ind.*, vol. 11, no. 1, pp. 20–31, Jan. 2014.
- [11] R. Suntivarakorn, and W. Treedet, "Improvement of boiler's efficiency using heat recovery and automatic combustion control system," *Energy Procedia*, vol. 100, pp. 193–197, Apr. 2016.
- [12] P. Dave, F. Desai, and H. Tailor H., "Energy conservation in bagasse fired boiler," *IJRITCC*, vol. 2, no. 9, pp. 2742–2745, Sep. 2014.
- [13] P. Kana-Donfack, C. Kapseu, D. Tchekam-Toko, and G. Ndong-Essengue, "Numerical modeling of sugarcane bagasse combustion in sugar mill boiler," *J. Energy Power Eng.*, vol. 13, pp. 80–90, Sep. 2019.
- [14] S. R. Arbaaz, W. V. Patil, and S. Panchal, "Review on boiler control automation for sugar industries," *Int. Res. J. Eng. Technol.*, vol. 4, no. 3, pp. 1928–1934, Apr. 2017.



- [15] J. R. Rodríguez Vazquez, R. Rivas-Perez, J. J. Sotomayor-Moriano, and J. R. Peran-González, "Advanced control system of the steam pressure in a fire-tube boiler," *IFAC Proc. Vol.*, vol. 41, no. 2, pp. 11028-11033, Jul. 2008.
- [16] B. W. Hogg, and N. M. El-Rabaie, "Multivariable generalized predictive control of a boiler system," *IEEE Trans. Energy Convers.*, vol. 6, no. 2, pp. 282-288, May 1991.
- [17] X. C. Dong, H. B. Wang, and X. X. Zhao, "Model reference neural network control for boiler combustion system," in *Proc. Fourth International Conference on Machine Learning and Cybernetics*, Guangzhou, China, 2005, vol. 8, pp. 4694-4698.
- [18] B. W. Hogg, and N. M. El-Rabaie, "Generalized predictive control of steam pressure in a drum boiler," *IEEE Trans. Energy Convers.*, vol. 5, no. 3, pp. 485-492, Jan. 1990.
- [19] J. Fessl, "An application of multivariable self-tuning regulators to drum boiler control," *Automatica*, vol. 22, no. 5, pp. 581-585, May 1986.
- [20] V. Havlena, and J. Findejs, "Application of model predictive control to advanced combustion control," *Control Eng. Prac.*, vol. 13, no. 6, pp. 671-680, Jun. 2005.
- [21] J. Zemse, A. Bhong, P. Patil, and S.V. Kulkarni "Sugar factory boiler automation," *Int. J. Sci. Tech. Adv.*, vol. 2, no. 2, pp. 107-109, Feb. 2016.
- [22] S. Wen, J. Yongcheng, "The research and application on intelligent control in boiler combustion system," *Procedia Eng.*, vol. 23, pp. 167-173, 2011.
- [23] S. R. Arbaaz, W. V. Patil, and S. Panchal, "Review on boiler control automation for sugar industries," *Inter. Res. J. Eng. Tech.*, vol. 04, no. 03, pp. 1928-1937, 2017.
- [24] T. G. Kao, M. Nguen, and R. Rivas-Perez, "Adaptive control of a delay plant by using a nonsearching self-adjusting system with a model," *Autom. Telemekh.*, no. 12, pp. 106-116, Dec. 1988.
- [25] I.O. Benitez, R. Rivas, V. Feliu, F.J. Castillo, "Temperature control based on a modified Smith predictor for injectable drug formulations," *IEEE Lat. Am. Trans.*, vol. 13, no. 41, pp. 1041-1047, Oct. 2015.
- [26] V. Feliu-Batlle, and R. Rivas-Perez, "Control of the temperature in a petroleum refinery heating furnace based on a robust modified Smith predictor," *ISA Trans.*, DOI: 10.1016/j.isatra.2020.12.006, 2020.
- [27] C. A. Monje, Y. Q. Chen, B. M. Vinagre, D. Y. Xue, and V. Feliu, *Fractional-order systems and controls. Fundamentals and applications*, London, UK: Springer, 2010.
- [28] L. Podlubny, *Fractional differential equations*, San Diego, USA: Academic Press, 1999.
- [29] Y. Chen, B. M. Vinagre, and I. Podlubny, "Continued fraction expansion approaches to discretizing fractional order derivatives an expository review," *Nonlinear Dyn.*, vol. 38, no. (1-4), pp. 155-170, Sep. 2004.
- [30] Y. Chen, and K. L. Moore, "Analytical stability bound for a class of delayed fractional-order dynamic systems," *Nonlinear Dyn.*, vol. 29, no. 1, pp. 191-200, Jan. 2002.
- [31] I. Petras, and L. Dorcak, "The frequency method for stability investigation of fractional control systems," *J. SACTA*, vol. 2, no. 1-2, pp. 75-85, Jan. 1999.
- [32] A. Oustaloup, O. Cois, P. Lanusse, P. Melchior, X. Moreau, and J. Sabatier, "The crone approach: Theoretical developments and major applications," *IFAC Proc. Vol.*, vol. 39, no. 11, pp. 324-354, Nov. 2010.
- [33] S. N. Calderon-Valdez, V. Feliu-Batlle, and R. Rivas-Perez, "Fractional-order mathematical model of an irrigation main canal pool," *Span. J. Agric. Res.*, vol. 13, no. 3, e0212, Apr. 2015.
- [34] F. J. Castillo, V. Feliu, R. Rivas, and L. Sanchez, "Design of a class of fractional controllers from frequency specifications with guaranteed time domain behavior," *Comput. Math. with Appl.*, vol. 59, no. 5, pp. 1656-1666, May 2010.
- [35] F. Castillo-Garcia, V. Feliu-Batlle, and R. Rivas-Perez, "Frequency specifications regions of fractional-order PI controllers for first order plus time delay processes," *J. Process Control*, vol. 23, no. 4, pp. 598-612, Apr. 2013.
- [36] B. M. Vinagre, C. A. Monje, A. J. Calderon, and J. I. Suarez, "Fractional PID controllers for industry application. A brief introduction," *J. Vib. Control*, vol. 13, no. (9-10), pp. 1419-1429, Nov. 2007.
- [37] V. Feliu-Batlle, R. Rivas-Perez, and F. J. Castillo-García, "Simple fractional order controller combined with a Smith predictor for temperature control in a steel slab reheating furnace," *International Journal of Control, Automation and Systems*, vol. 11, no. 3, pp. 533-544, June 2013.
- [38] R. Rivas-Perez, F. Castillo-Garcia, J. Sotomayor-Moriano, and V. Feliu-Batlle, "Design of a fractional order PI controller for steam pressure in the steam drum of a bagasse fired boiler," *IFAC Proc. Vol.*, vol. 47, no. 33, pp. 1337-1342, Sep. 2014.
- [39] Y. Luo, Y. Q. Chen, C. Y. Wang, and Y. G. Pi, "Tuning fractional order proportional integral controllers for fractional order systems," *J. Process Control*, vol. 20, no. 7, pp. 823-831, Jul. 2010.
- [40] I. Birs, C. Muresan, I. Nascu, and C. Ionescu, "A survey of recent advances in fractional order control for time delay systems," *IEEE Access*, vol. 7, pp. 30951-30965, Jul. 2019.
- [41] J. Z. Shi, "A fractional order general Type-2 fuzzy PID controller design algorithm," *IEEE Access*, vol. 8, pp. 52151-52172, Aug. 2020.
- [42] Y. Luo, Y. Q. Chen, C. Y. Wang, and Y. G. Pi, "Tuning fractional order proportional integral controllers for fractional order systems," *J. Process Control*, vol. 20, no. 7, pp. 823-831, Aug. 2010.
- [43] M. Bettayeb, and R. Mansouri, "Fractional IMC-PID-filter controllers design for non integer order systems," *J. Process Control*, vol. 24, no. 4, pp. 261-271, Apr. 2014.
- [44] A. C. Agüero, J. R. Pisa, C. J. Agüero, and A. T. Bugeau, "Poder calorífico del bagazo de caña de azúcar," *Revista de Ciencias Exactas e Ingeniería*, vol. 13, no. 24, pp. 33-37, Oct. 2004.
- [45] K. J. Astrom, and R. D. Bell, "Drum-boiler dynamics," *Automatica*, vol. 36, no. 3, pp. 363-378, Apr. 2000.
- [46] F. De Mello, "Boiler models for system dynamic performance studies," *IEEE Trans. Power Syst.*, vol. 6, no. 1, pp. 66-74, Jan. 1991.
- [47] G. Pellegrinetti, and J. Bentsman, "Nonlinear control oriented boiler modeling a benchmark problem for controller design," *IEEE Trans. Control Syst. Technol.*, vol. 4, no. 1, pp. 57-64, Jan. 1996.
- [48] L. Ljung L. (1999). *System identification - theory for the user's*, second edition, New Jersey, N.J., USA: Prentice Hall, 1996.
- [49] R. Rivas-Perez, V. Feliu-Batlle, F. J. Castillo-Garcia, and A. Linares-Saez, "Mathematical model for robust control of an irrigation main canal pool," *Environ. Model. Soft.*, vol. 51, pp. 207-220, Sep. 2014.
- [50] K. Ogata, *Modern control engineering*, fourth edition, Madrid, Spain: Pearson Education S.A., 2003.



**VICENTE FELIU-BATLLE** received his M.Sc (with honors) in industrial engineering and a PhD from the Polytechnical University of Madrid, Spain in 1979 and 1982 respectively. He also holds and MSc in physics (1986). He was Dean of the School of Industrial Engineering at the Universidad de Castilla la Mancha, Spain from 1994 to 2008. Currently he is leading the Automation and Robotics Group at the same university. His research interests include multivariable and digital control systems, fractional dynamics and control, kinematic and dynamic control of rigid and flexible robots and computer vision for robots. He is a senior member of the IEEE and a member of IFAC.



**RAUL RIVAS-PEREZ** received his Engineering and the M.Sc (with honors) degrees in Automatic Control from the Odessa Polytechnic University, Ukraine in 1979, and the PhD and the Doctor Science (DSc) degrees from the Institute of Hydraulic Engineering and Land Reclamation of Ukrainian Academy of Agrarian Sciences in 1984 and 1990 respectively. He has been a full-time professor at the Havana Technological University since 1992. Currently he is the leading of Advanced Control Systems Group at the same university. His research interests include identification and advanced control of complex and uncertain dynamic processes, fractional order dynamics and control, system identification for robust control, robust control of large time-delay systems.





**FERNANDO CASTILLO GARCÍA** received his degree in Industrial Engineering and his PhD in Mechatronics from University of Castilla-La Mancha in 2000 and 2010, respectively. He has been teaching assistant in University of Castilla-La Mancha since 2000, and since 2018 he works in School of Industrial and Aerospace Engineering at the Universidad de Castilla la Mancha, Spain developing research projects

with the industry. His research interests include fractional calculus and control, control and modeling of flexible manipulators and motion control.